Dedicated to Professor Dumitru Oancea
on the occasion on his 75th anniversary

MESOPOROUS SILICA-CERIA COMPOSITES AS CARRIERS FOR DRUG DELIVERY SYSTEMS

Marilena PETRESCU,[a] Raul-Augustin MITRAN,[a,b] Cristian MATEI[a] and Daniela BERGER[a]*

[a]University "Politehnica" of Bucharest, Faculty of Applied Chemistry and Material Science, Bucharest, Polizu no. 1-7, Bucharest, 011061, Roumania
[b]Roumanian Academy, Institute of Physical-Chemistry "Ilie Murgulescu", 202 Splaiul Indepedentei, Bucharest, 060021, Roumania

The paper presents the synthesis and characterization of mesoporous silica-ceria composites with an ordered hexagonal pore array characteristic for MCM-41 materials, which were applied as carriers for oxytetracycline, an antibiotic active against a broad range of Gram-negative and Gram-positive bacteria. The mesoporous matrices and antibiotic-loaded samples were characterized by various techniques: small- and wide-angle XRD, FTIR spectroscopy, N_2 adsorption-desorption isotherms, SEM and TEM. The drug delivery profiles were determined in saline buffer phosphate solution, pH=5.7 by using UV-vis spectroscopy. All drug release profiles exhibited a pronounced burst effect, but slower kinetics was noticed for oxytetracycline delivered from mesoporous silica-ceria composites.
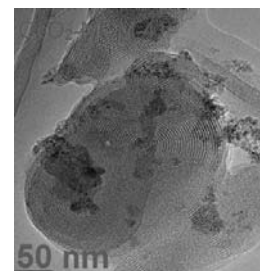
INTRODUCTION

The design of functional materials for biomedical applications has focused many research efforts. Among inorganic materials tested as vehicles in drug delivery systems, ordered mesoporous silica has received a lot of interest,[1-5] since 2001 when MCM-41 silica matrix was reported as carrier for ibuprophen[3] due to its outstanding properties: ordered pore array with tunable pore dimension, high surface area and total pore volume, as well as biocompatibility. Nonporous and nonordered porous colloidal silica materials are accepted as excipients in pharmaceutical formulations, being listed in the Inactive Ingredients Database of U.S. Food and Drug Administration.[1]

Recently, several studies reported interactions between mesoporous silica nanoparticles (MSN) and biological systems, inorganic nanoparticles being transported into cells through endocytosis that occurs through either specific or nonspecific cellular uptake depending on MSN properties (shape, size and surface properties). Tremendous efforts have focused on the synthesis of uniform-sized and shaped dispersible MSN with tunable pore size that can accommodate enough high content of pharmaceutical active ingredient.[5,6]

Ceria possesses a cubic fluorite structure that tends to be a nonstoichiometric compound due to its dual oxidation state of cerium atoms, +4 and +3, which means that the reduction of Ce^{4+} to Ce^{3+} is accompanied by formation of oxygen vacancies,

---

* Corresponding author: danaberger01@yahoo.com

responsible for its catalytic and antioxidant properties. Based on X-ray photoelectron spectroscopy and X-ray absorption near edge spectroscopy studies one can conclude that the concentration of Ce^{3+} relative to Ce^{4+} increases with the particle size decrease, with a Ce^{3+} content of minimum 6% in 6 nm nanoparticles and 1% in 10 nm particles.[7]

Nanoceria exhibits radical scavenger properties in cell cultures as consequence of interconversion of $Ce^{4+} \leftrightarrow Ce^{3+}$ on nanoparticles surface acting as superoxide dismutase and catalase mimetic.[8] Based on its ability to scavenge free radicals, nanoceria could be applied as therapeutic agent for: the decrease of retinal degeneration, the reduction of superoxide and peroxynitrite formation in ischemic cardiomyopathy, the treatment of neurological diseases.[8-10] Andreescu *et al.* reported a strong attachment of dopamine to the ceria nanoparticles surface resulting from charge transfer complexes. This process involves the oxidation of dopamine by CeO_2 to dopaquinone intermediates and the attachment of quinonic moiety to ceria surface lowering the free dopamine level in biological systems exposed to nanoceria.[11]

As drug vehicle, ordered mesoporous silica could be combined in a composite or hybrid material with inorganic or organic compound, in order to design advanced functional materials that gather the advantages of both components of the composite. Herein, we report the synthesis of mesoporous silica-ceria composites that were employed as carriers in drug delivery systems using a model molecule, oxytetracycline, and compared with MCM-41 silica material.
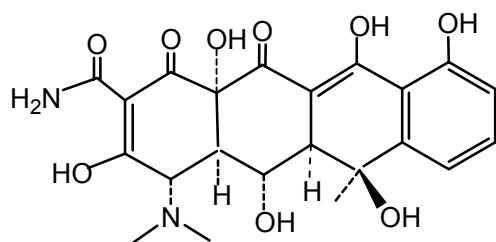

Fig. 1 – The chemical structure of oxytetracycline.

Oxytetracycline (Fig. 1) is a broad spectrum antibiotic with activity against various bacteria that is still used to treat infections. It is administered by oral route and is partially absorbed in the gastrointestinal tract.[12] Recently, oxytetracycline-loaded MCM-41 silica and aluminosilicates proved to have good bactericidal activity against *Staphylococcus aureus* ATCC43300.[13]

EXPERIMENTAL

1. Synthesis of mesoporous silica-ceria composites

Mesoporous silica-ceria composites containing 10% and 20% (mol) ceria nanoparticles were prepared by sol-gel method using tetraethyl orthosilicate (TEOS, Fluka) as silicon source and ammonium cerium(IV) nitrate ($(NH_4)_2Ce(NO_3)_6$, Sigma-Aldrich) as ceria precursor, in the presence of cetyl trimethylammonium bromide (CTAB, Alfa Aesar), in basic medium. To the aqueous solution of CTAB, 25% ammonia aqueous solution (Scharlau) was added and when the reaction mixture reached 40°C, TEOS was added dropwise. After precipitation, aqueous solution of ammonium cerium(IV) nitrate was added. The molar ratios, TEOS : $(NH_4)_2Ce(NO_3)_6$: CTAB : NH_3 were 1:0.1:0.25:3.37 for $MCM-CeO_2(1)$ containing 10%(mol) ceria nanoparticles and 1:0.2:0.27:3.7 for $MCM-CeO_2(2)$ with 20%(mol) CeO_2, respectively. The reaction mixture was ageing under vigorous magnetic stirring at 60°C/1h for a good impregnation of colloidal silica with cerium ions and then was hydrothermally treated at 100 °C, 96 h in a teflon-lined autoclave under autogeneous pressure in static conditions. The solids were filtered off, washed with ethanol and warm water and dried at room temperature. In order to remove the structure directing agent (CTAB), a calcining step at 550°C/5h with a heating rate of 1°C/min was performed.

For comparison, a MCM-41 silica sample was prepared according to a reported procedure.[14] For the surfactant removal, a two-steps procedure was carried out. Firstly, 1 g of silica sample was refluxed in 100 mL ethanol solution containing 2 g of ammonium nitrate at 90 °C for 1h and then the solid was filtered off, washed and dried. A second refluxing step in acidic alcoholic solution (9 mL HCl 37% in 100 mL ethanol) at 90°C for 1h was performed.[15] The MCM-41 sample treated in such way was denoted MCM-41E. Also, in this study the calcined (550°C/5h) MCM-41 sample was used.

2. Drug loading and *in vitro* release studies

Drug loading was carried out by incipient wetness impregnation method. To an oxytetracycline hydrochloride (Sigma) aqueous solution of 100 mg/mL concentration, 100 mg inorganic carrier was added, gently stirred and dried under vacuum at room temperature, in dark conditions, for 8 h. The resulted drug-loaded samples were labeled oxy(content%wt)@support.

In vitro drug delivery experiments were performed in saline phosphate buffer solution (PBS, *p*H 5.5) at 37 °C, under magnetic stirring (150 rpm). An amount of oxytetracycline-loaded sample containing 12.5 mg drug was suspended into 90 mL PBS. Aliquots were periodically withdrawn, properly diluted and analyzed by UV-VIS spectroscopy (Ocean Optics USB 4000 spectrometer).

Both inorganic supports and oxytetracycline-loaded samples were characterized by FTIR spectra recorded in the wavenumber range of 4000-200 cm^{-1} using CsI pellet technique (Bruker Tensor 27 spectrometer), small- and wide-angle XRD (Rigaku Miniflex II diffractometer), N_2 adsorption/desorption isotherms performed at 77 K (Quantachrome Autosorb iQ$_2$ porosimeter), TEM (FEI Tecnai G2-F30) and SEM (Tescan Vega 3 LM).

RESULTS AND DISCUSSION

The wide-angle XRD patterns of both silica-ceria composites evidenced the presence of fluorite phase with cubic symmetry characteristic to ceria

nanoparticles, besides the amorphous silica phase (Fig. 2A). The small-angle XRD results proved the formation of an ordered hexagonal pore array, both composite samples exhibiting the Bragg reflections characteristic to MCM-41 materials (Fig. 2B), higher intensity can be observed for the composite with lower content of ceria nanoparticles. The MCM-41 samples exhibited a highly-ordered 1D pore framework as small-angle XRD proved (Fig. 2B). No significant differences between small-angle XRD data of MCM-41 and MCM-41E (presented elsewhere[13]) were noticed.

In the FTIR spectra of inorganic mesoporous matrices one can notice the characteristic bands of silica and ceria: a large intense asymmetric and medium intense symmetric stretching vibrations at 1085 cm^{-1} and 800 cm^{-1} respectively, assigned to Si-O-Si bonds, at 960 cm^{-1} and 460 cm^{-1} indicating the presence of silanol groups and Si-O

deformation bands overlapped with very intense Ce-O band (Fig. 3).

The TEM investigation of MCM-CeO$_2$(1) composite showed an ordered pore array for silica phase, in agreement with small-angle XRD results, which presented spherical particles, while ceria phase was formed as very small nanocrystals with an average size of 5 nm that tended to be distributed in bundles (Fig. 4A). The SEM analysis of MCM-CeO$_2$(2) composite evidenced the formation of silica spherical particles with a diameter of 250-300 nm and small ceria nanoparticles on silica surface (Fig. 4B). The MCM-41 sample calcined at 550°C had bigger spherical particles than the composite samples with the diameter ranging between 400-600 nm (Fig. 4C), while the MCM-41E sample exhibited spherical particles associated in rods, preserving the morphology of surfactant micelles (Fig. 4D) as SEM investigation proved.
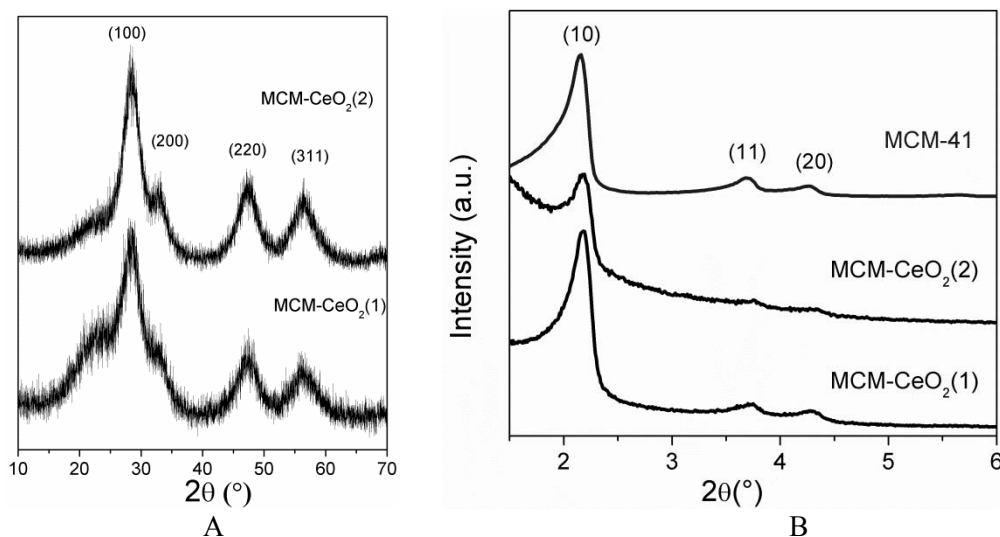

Fig. 2 – XRD patterns of silica-ceria composites calcined at 550°C/5h: wide angle (A) and small angle in comparison with MCM-41 (B).
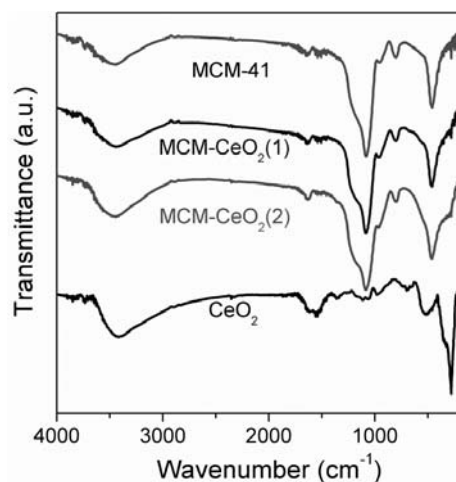

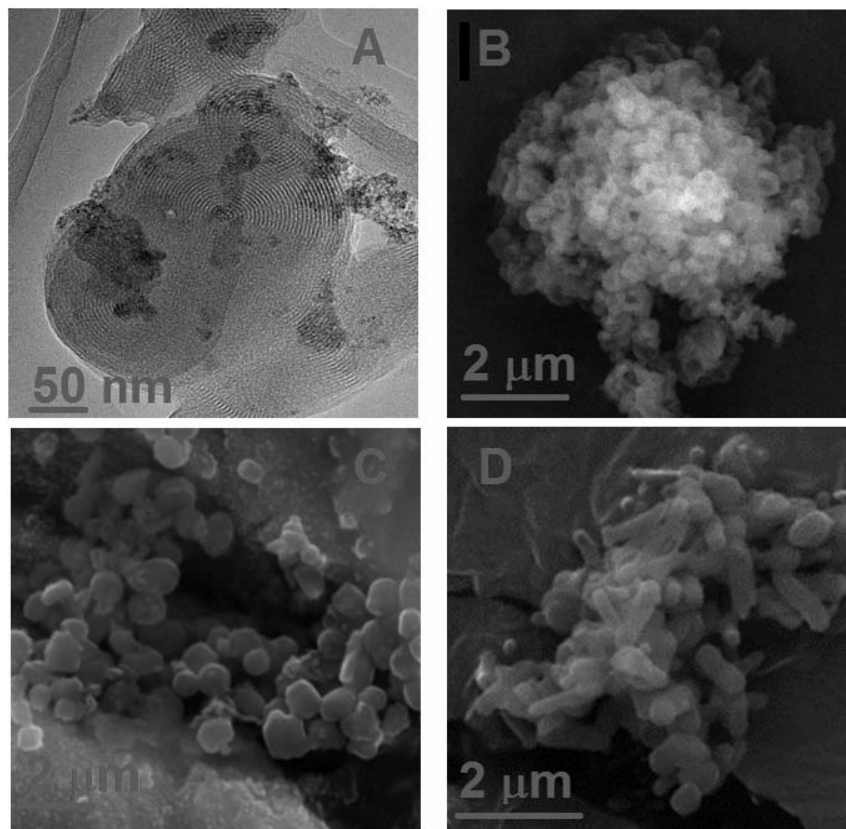Fig. 3 – FTIR spectra of silica-ceria composites in comparison with CeO$_2$ and MCM-41.

Fig. 4 – TEM image of MCM-CeO$_2$(1) (A) and SEM images of: MCM-CeO$_2$(2) (B), MCM-41 sample calcined at 550°C (C) and MCM-41E sample (D).
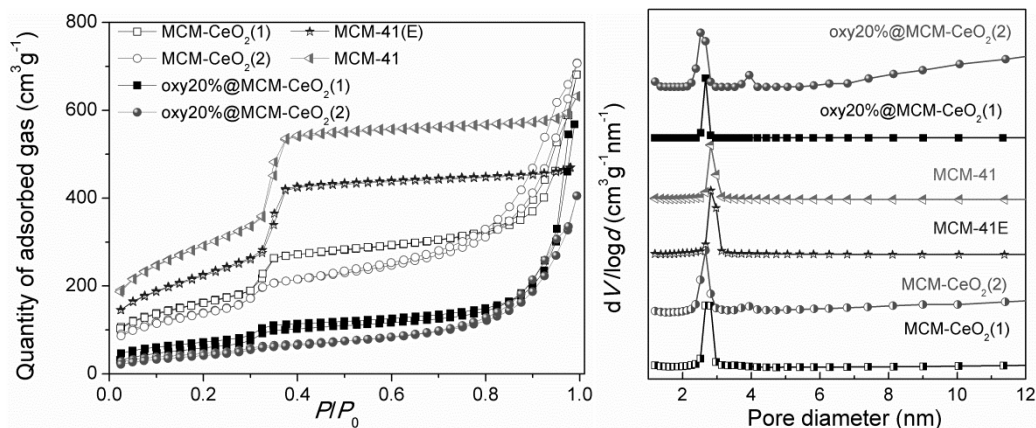

Fig. 5 – N$_2$ adsorption-desorption isotherms of synthesized supports and representative drug-loaded samples (A) and the corresponding pore size distributions (B).

The nitrogen adsorption-desorption isotherms of silica-ceria composites exhibited relative high porosity, being of type IV, characteristic for mesoporous materials (Fig. 5A). The specific surface area values (S_{BET}) were computed using Brunauer-Emmett-Teller method in the 0.05-0.30 relative pressure range and the pore size distribution curves were determined by Barrett-Joyner-Halenda model from desorption branch of isotherms; all samples presented unimodal pore

size distribution curves (Fig. 5B). The textural parameters (the specific surface area, S_{BET}, total pore volume, V_p and the average pore diameter, d_{BJH}) determined from N$_2$ adsorption-desorption isotherms of carriers were gathered in Table I. The porosity of the MCM-CeO$_2$(2) is lower than the other supports, having a fraction of macropores, explained by the presence of ceria nanoparticles on the silica particles surface (Fig. 5A and 5B). In comparison with MCM-41 sample, with the

average pore diameter, d_{BJH}, of 2.82 nm, the silica-ceria composites have slightly lower pore sizes (2.67 nm) (Table I).

The incipient wetness impregnation procedure was chosen to obtain oxytetracycline-loaded samples because it is a simple and reliable method, especially for highly soluble drugs with a low chemical stability. Oxytetracycline was loaded onto the silica-ceria composites, as well as on pristine MCM-41 samples taking into account the inorganic support porosity.

The presence of oxytetracycline molecules loaded onto the inorganic supports was indicated by FTIR spectroscopy. In the FTIR spectra of drug-loaded samples it can be observed the vibration bands that belong to the support, besides the ones of the drug located in the range of: 2850-2950 cm^{-1} attributed to $\upsilon_{as,s}$(CH)), 1590-1650 cm^{-1} ascribed to the deformation of amide moieties and 1310-1410 cm^{-1} assigned to the phenol groups (Fig. 6).

The recorded N$_2$ adsorption-desorption isotherms for oxytetracycline-loaded materials showed a lower porosity (lower values of specific surface area and mesopores volume) than of the corresponding supports (Fig. 5A), the textural parameters of the oxytetracycline-based samples being listed in Table I. Only a slight decrease of the average pore size was observed that means weak interactions between drug molecules and inorganic matrix were established (Fig. 5B).

In the wide-angle XRD patterns of the oxytetracycline-loaded samples (Fig. 7), only the Bragg reflection of fluorite phase can be noticed, demonstrating that the antibiotic molecules were adsorbed into the carrier mesopores in amorphous state. The lack of the drug diffraction peaks suggested that no crystalline oxytetracycline was present in all drug-loaded supports, as it was expected.
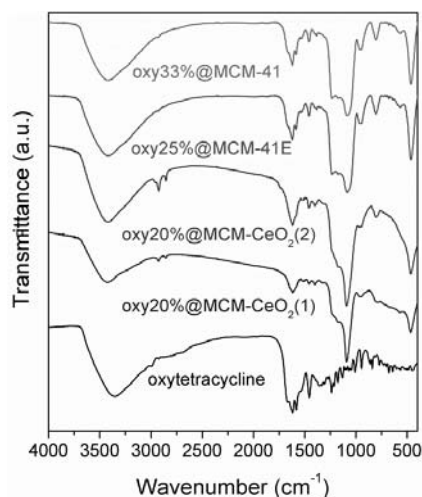

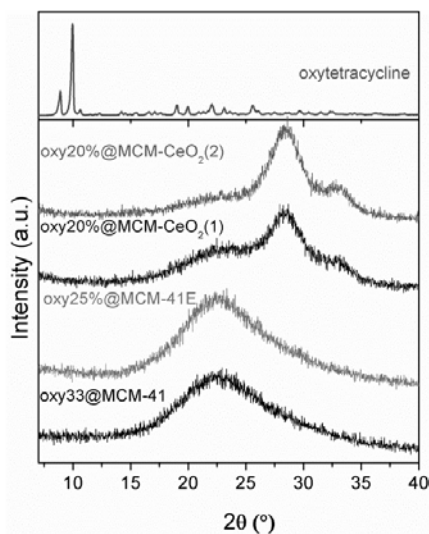Fig. 6 – FTIR spectra of oxytetracycline and oxytetracycline-loaded supports.

Fig. 7 – Wide-angle XRD patterns of oxytetracycline and loaded supports.

Table 1

Textural properties of carriers and drug-loaded samples

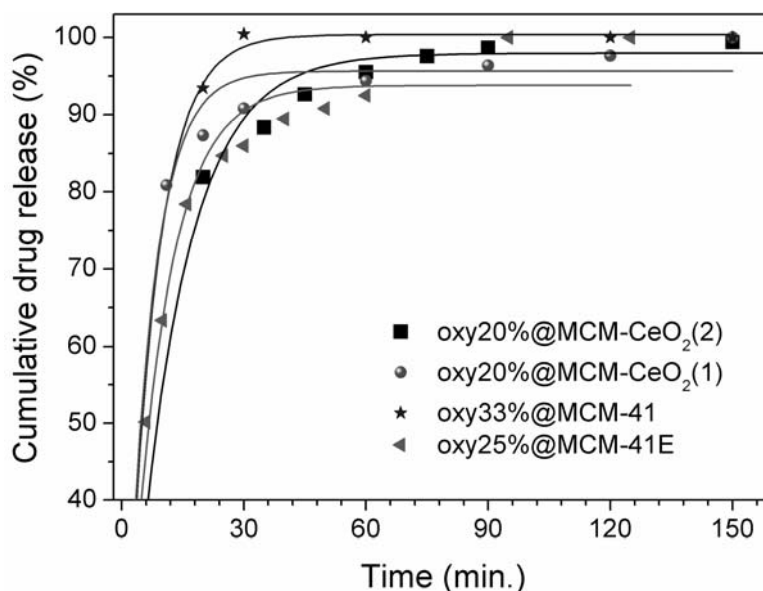| Samples	S_{BET} (m²/g)	V_p (cm³/g)	d_{BJH} (nm)	Period of drug total release (min.)
MCM-CeO$_2$(1)	683	0.67	2.66	
MCM-CeO$_2$(2)	512	1.14	2.67	
MCM-41E	819	0.73	2.81	
MCM-41	1045	1.06	2.82	
oxy20%@MCM-CeO$_2$(1)	265	0.05 (d_p< 10 nm)	2.64	150
oxy20%@MCM-CeO$_2$(2)	173	0.04 (d_p< 10 nm)	2.52	150
oxy25%@MCM-41E	144	0.12 (d_p< 10 nm)	2.81	95
oxy33%@MCM-41	163	0.10 (d_p< 10 nm)	2.80	60

Fig. 8 – The oxytetracycline cumulative release profiles from silica-ceria composites in comparison with MCM-41 samples.

In vitro oxytetracycline release experiments were performed in saline phosphate buffer solution at *p*H 5.7 as simulated body fluid. Oxytetracycline, very soluble in water, has low photochemical and chemical stability, especially in basic solutions. From all studied carriers, the antibiotic molecules were completely delivered within a period between 60 to 150 min. (Table I), all release profiles exhibiting a pronounced burst effect (Fig. 8).

The drug delivery from silica-ceria composites was slightly slower than from MCM-41. The higher content of silanol groups in MCM-41E slows down the antibiotic delivery kinetics in comparison with the corresponding calcined MCM-41 carrier. Recently, we reported a similar behavior for doxycycline that had a slower release kinetics from MCM-CeO$_2$(1) than MCM-41 silica matrix.[16]

CONCLUSIONS

We successfully obtained silica-ceria composites having an ordered hexagonal pore array characteristic to MCM-41 materials and relatively high porosity. The composite materials were used as carriers for oxytetracycline and compared with MCM-41-type silica support.

The antibiotic molecules were loaded into the mesopores of inorganic material in amorphous state. The drug delivery kinetics was slower from silica-ceria composites than from MCM-41, from all studied vehicles, oxytetracycline being completely recovered in 150 min. for silica-ceria composites and in 60 min. from MCM-41. Regarding the silica matrix, the uncalcied sample led to a slower drug release than the calcined MCM-41 support.

REFERENCES

1. T. Limnell, H.A. Santos, E. Makila, T. Heikkila, J. Salonen, D.Y. Murzin, N. Kumar, T. Laaksonen, L. Peltonen and J. Hirvonen, *J. Pharm. Sci.*, **2011,** *100*, 3294-3006,

2. Y.S. Lin and C.L. Haynes, *Chem. Mater.*, **2009**, *21*, 3979–3986.

3. M. Vallet-Regi, A. Ramilla, R.P. del Real and J. Perez-Pariente, *Chem. Mater.*, **2001**, *13,* 308-311.

4. S.H. Wu, Y. Hung and C.Y. Mou, *Chem. Commun.*, **2011***, 47*, 9972–9985.

5. B.G. Trewyn, J.A. Nieweg, Y. Zhao, V. S. Y. Lin, *Chem. Eng. J.,* **2008**, *137*, 23–29.

6. X. Huang, X. Teng D. Chen, F. Tang, J. He, *Biomaterials,* **2010**, *31*, 438–448.

7. D. Schubert, R. Dargusch, J. Raitano and S.W. Chan, *Biochem. Biophys. Res. Com.*, **2006**, *42*, 86–91.

8. L. Kong, X. Cai, X.H. Zhou, L.L. Wong, A.S. Karakoti, S. Seal and J.F. McGinnis, *Neurobiol Dis.*, **2011**, *42*, 514-523.

9. J.L. Niu, A. Azfer, L.M. Rogers, X.H. Wang and P.E. Kolattukudy, *Cardiovasc. Res.,* **2007**, *73*, 549–559.

10. C. K. Kim, T. Kim, I.-Y. Choi, M. Soh,. Dg Kim, Y.-Ju Kim, H. Jang, H-S. Yang, J. Y. Kim, H.K. Park, S. P. Park, S. Park, T. Yu, B.-W. Yoon, S.-H. Lee and T. wan Hyeon, *Angew. Chem. Int. Ed.,* **2012**, *51*, 11039-11043.

11. Hayat, D. Andreescu, G. Bulbul and S. Andreescu, *J. Coll. Inter. Sci.*, **2014**, *418*, 240–245.

12. E.C. Perreira-Maia, P.P. Silva, W.B. De Almeida, H.F. Dos Santos, B.L. Marcial, R. Ruggeiro and W. Guerra, *Quimica Nova*, **2010**, *33*, 700-706.

13. D. Berger, S. Nastase, R.A. Mitran, M. Perescu, E. Vasile, C. Matei and T Negranu-Pirjol, *Int. J. Pharm.*, **2016**, *510*, 524-531.

14. D. Berger, L. Bajenaru, S. Nastase, R.A. Mitran, C. Munteanu and C. Matei, *Micropor. Mesopor. Mater.,* **2015**, *206*, 150–160.

15. J. Kecht and T. Bein, *Micropor. Mesopor. Mater.,* **2008**, *116*, 123–130.

16. M. Petrescu, R.A. Mitran, A.M. Luchian, C. Matei and D. Berger, *U.P.B. Sci. Bull., Series B*, **2015**, *77* 13-24.